Author Manuscript

Author Manuscript

Author Manuscript

Author Manuscript

HHS Public Access

Author manuscript

Oncogene. Author manuscript; available in PMC 2011 June 09.

Published in final edited form as:

Oncogene. 2010 December 9; 29(49): 6485–6498. doi:10.1038/onc.2010.377.

Transforming Growth Factor-β-Induced Epithelial-Mesenchymal Transition Facilitates Epidermal Growth Factor-Dependent Breast Cancer Progression

Michael K. Wendt, PhD, **Jason A. Smith, BS**, and **William P. Schiemann, PhD**

Case Comprehensive Cancer Center, Case Western Reserve University, Wolstein Research Building, 2103 Cornell Road Cleveland, OH 44106

Abstract

TGF-β and EGF play critical roles in regulating the metastasis of aggressive breast cancers, yet the impact of epithelial-mesenchymal transition (EMT) induced by TGF-β in altering the response of breast cancer cells to EGF remains unknown. We show here that murine metastatic 4T1 breast cancer cells formed compact, and dense spheroids when cultured under 3-dimensional (3D) conditions, which contrasted sharply to the branching phenotypes exhibited by their nonmetastatic counterparts. Using the human MCF10A series, we show that epithelial-type and nonmetastatic breast cancer cells were unable to invade to EGF, while their mesenchymal-type and metastatic counterparts readily invaded to EGF. Furthermore, EMT induced by TGF-β was sufficient to manifest spheroid morphologies, a phenotype that increased primary tumor exit and invasion to EGF. Post-EMT invasion to EGF was dependent upon increased activation of EGFR and p38 MAPK, all of which could be abrogated either by pharmacological (PF-271) or genetic (shRNA) targeting of focal adhesion kinase (FAK). Mechanistically, EMT induced by TGF-β increased cell surface levels of EGFR and prevented its physical interaction with E-cadherin, leading instead to the formation of oncogenic signaling complexes with TβR-II. Elevated EGFR expression was sufficient to transform normal mammary epithelial cells, and to progress their 3D morphology from that of hollow acini to branched structures characteristic of nonmetastatic breast cancer cells. Importantly, we show that TGF-β stimulation of EMT enabled this EGFR-driven breast cancer model to abandon their inherent branching architecture and form large, undifferentiated masses that were hyper-invasive to EGF and displayed increased pulmonary tumor growth upon tail vein injection. Finally, chemotherapeutic targeting of FAK was sufficient to revert the aggressive behaviors of these structures. Collectively, this investigation has identified a novel EMT-based approach to neutralize the oncogenic activities of EGF and TGF-β in aggressive and invasive forms of breast cancer.

Users may view, print, copy, download and text and data- mine the content in such documents, for the purposes of academic research, subject always to the full Conditions of use: http://www.nature.com/authors/editorial_policies/license.html#terms

Corresponding Author: William P. Schiemann, Case Comprehensive Cancer Center, Case Western Reserve University, Wolstein Research Building, 2103 Cornell Road Cleveland, OH 44106 Phone: 216-368-5763. Fax: 216-368-1166. william.schiemann@case.edu.

CONFLICT OF INTEREST

The authors declare no conflict of interest

Supplementary information is available at Oncogene's website.

Author Manuscript Author Manuscript Author Manuscript Author Manuscript

Keywords

EGFR; TGF-β; FAK; breast cancer; metastasis; invasion

INTRODUCTION

The process of epithelial-mesenchymal transition (EMT) induced by transforming growth factor-b (TGF-β) is well established as a critical mechanism of tumor progression (Kalluri and Weinberg, 2009; Moustakas and Heldin, 2007; Wendt *et al.*, 2009a; Zavadil and Bottinger, 2005); however, how these TGF-β-dependent events impact the response to growth factors during metastasis remains incompletely understood (Cowin and Welch, 2007; Moustakas and Heldin, 2007; Wendt *et al.*, 2009a). Equally mysterious are the reasons underlying the failure of science and medicine to readily detect the classical mesenchymal and sarcomatoid phenotypes exhibited by fully transitioned carcinoma cells at sites of secondary metastases, which in theory should be enriched in these dedifferentiated and post-EMT cell types (Tarin *et al.*, 2005). It therefore stands to reason that deciphering the molecular mechanisms that underlie the interplay between EMT and its counterpart mesenchymal-epithelial transition (MET) (Hugo *et al.*, 2007), may offer new inroads into targeting tumor metastasis.

Applying genomic analyses to human breast cancers has resulted in the identification and classification of at least five genetically distinct breast cancer subtypes (Perou *et al.*, 2000; Sorlie *et al.*, 2001; Sorlie *et al.*, 2003), of which the basal-like “triple-negative” subtype remains the most intractable to clinical intervention. More recently, elevated expression of ErbB1/EGF receptor (EGFR) in basal-like tumors has been identified as a highly predictive marker for poor clinical outcomes (Tischkowitz *et al.*, 2007) Indeed, synergistic activity between TGF-β and EGF in stimulating EMT has been identified (Saha *et al.*, 1999), while the actual process of EMT has been associated with the development of chemoresistance to EGFR-targeted therapies in carcinoma cells (Barr *et al.*, 2008; Buck *et al.*, 2007; Thomson *et al.*, 2005; Thomson *et al.*, 2008). Because TGF-β is a master regulator of EMT, we hypothesized that EMT stimulated by TGF-β would induce a fundamental change in how tumor cells sense and respond to their surrounding microenvironment, particularly to EGF (Joo *et al.*, 2007; Wang *et al.*, 2009). Along these lines, recent studies suggest that aberrant EGFR signaling reflects the inactivation of E-cadherin, the hallmark of EMT (Bremm *et al.*, 2008; Miettinen *et al.*, 1994; Takahashi and Suzuki, 1996; Wilding *et al.*, 1996). However, other studies implicate a novel paracrine signaling loop that transpires between carcinoma cells and tumor-infiltrating macrophages that comprises the actions of TGF-β, EGF, and CSF-1 in promoting breast cancer cell migration and invasion to EGF (DeNardo *et al.*, 2009; Wyckoff *et al.*, 2004; Wyckoff *et al.*, 2000).

Focal adhesion kinase (FAK) is a multifunctional protein tyrosine kinase and scaffolding molecule that links transmembrane signaling inputs arising from integrins and growth factor receptors to intracellular effectors (Mitra *et al.*, 2006). Along these lines, FAK has been shown to interact directly with the intracellular domain of EGFR to facilitate its downstream signaling and activation of cell motility (Sieg *et al.*, 2000). Recently, analyses by our

Author Manuscript Author Manuscript Author Manuscript Author Manuscript

laboratory established a key role for FAK in physically associating integrins with TβR-II (Wendt and Schiemann, 2009). Moreover, we demonstrated that the chemotherapeutic targeting of FAK prevented the infiltration of macrophages into primary mammary tumors (Wendt and Schiemann, 2009). Clearly, these and other studies have established FAK as a key player in mediating EMT and metastasis stimulated by TGF-β (Cicchini *et al.*, 2008; Ding *et al.*, 2008); however, whether FAK facilitates the potential pathophysiological activities between TGF-β and EGF remains unknown. Thus, the objectives of the present study were to *(i)* determine how the response of mammary epithelial cells (MECs) to EGF was altered by EMT induced by TGF-b; *(ii)* establish the signaling mechanisms responsible for eliciting the aberrant responses of post-EMT MECs to EGF; and *(iii)* characterize the 3D morphology of resulting hyper-invasive, post-EMT MECs.

RESULTS

Metastatic breast cancer cells grow as dense cell structures manifested by TGF-βinduced EMT

Recent studies strongly suggest that the morphology and cell signaling responses of mammary tumors are more accurately recapitulated *in vitro* using three dimensional (3D) organotypic systems as compared to growing cells on plastic (CC Park, 2000; Kenny *et al.*, 2007; Wendt *et al.*, 2009b). To this end, we utilized a well-characterized murine mammary carcinoma progression series comprised of several isogenic cell lines that possess varying metastatic proficiencies and include: *(i)* noninvasive and nonmetastatic 67NR cells, which form primary tumors that cannot enter the circulation; *(ii)* invasive and nonmetastatic 4T07 cells, which traverse the circulation and fail to establish secondary tumors in the lung; and *(iii)* highly metastatic 4T1 cells, which disseminate widely and colonize multiple organ sites (Aslakson and Miller, 1992). Somewhat surprisingly, both nonmetastatic cell lines formed highly branched 3D structures, while the metastatic 4T1 cells formed dense spheroids to lobular-like structures that were devoid of branching (Figure *1a*). To verify the metastatic designation of these MEC derivatives, we engineered them to stably express luciferase and then engrafted them onto the mammary fat pad and pulmonary metastasis was tracked over time using bioluminescent imaging (Figure *1b*). Given the recent studies from our lab and others identifying a critical role of EMT in driving breast cancer progression, we sought to examine how EMT induced by TGF-β affected subsequent 3D culture morphologies and tumor metastasis (Padua *et al.*, 2008; Wendt and Schiemann, 2009; Wendt *et al.*, 2009a). Interestingly, following a prolonged treatment with TGF-β, 4T07 cells displayed a 3D morphology that was highly reminiscent of the metastatic 4T1 cells (Figure *1c* and *1a*). To verify their EMT status, lysates of TGF-β treated 4T07 cells were analyzed for decreased expression of E-cadherin and increased expression of Vimentin (Figure *1d*). Given the somewhat counterintuitive nature of this TGF-β-induced 3D EMT morphology, we utilized the 67NR cell line that grew as a mixture of independent spheroid and branched structures (Supplementary Figure 1). Indeed, by physically isolating the spheroid structures from 3D-cultures, expanding them on a plastic growth surface and then placing them back into 3D-cultures we definitively showed that spheroid structures in 3D-cultures directly correspond to a classic mesenchymal morphology when cultured plastic (Supplementary Figure 1). Recent studies indicate a prominent role for paracrine EGF production in driving breast

Author Manuscript Author Manuscript Author Manuscript Author Manuscript

cancer metastasis (DeNardo *et al.*, 2009; Wyckoff *et al.*, 2004). Therefore, we hypothesized that post-EMT breast cancer cells would be hyper-invasive in response to EGF as compared pre-EMT cells. Indeed, control 4T07 cells, although highly invasive in response to serum, exhibited little-to-no invasion specifically in response to EGF (Figure *1e*). In contrast, post-EMT 4T07 cells readily invaded in response to a solitary EGF stimulus (Figure *1e*). Furthermore, and consistent with the establishment of paracrine EGF signaling axes in regulating breast cancer metastasis (Wyckoff *et al.*, 2004), we observed significantly elevated quantities of post-EMT 4To7 cells in the lungs of mice at 2 and 4 weeks post-engraftment onto the mammary fat pad (Figure *1f*). Although the ultimate fate of disseminated post-EMT cells cannot be ascertained from this experiment, our findings nonetheless show the *(i)* importance of EMT to enhance metastatic seeding, and *(ii)* the inability of EMT to sustain secondary tumor growth (Figure *1f*). Consistent with these findings epithelial-type and nonmetastatic human MCF-7 and MCF10AT1K cells failed to invade in response to EGF while their mesenchymal-type and malignant human MDAMB-231 and MCF10A-CA1h counterparts readily invaded in response to EGF (Supplementary Figure 2). Collectively, these findings strongly suggest that the process of EMT facilitates the ability of human breast cancer cells to invade aberrantly in response to EGF.

TGF-β stimulation of EMT results in the generation of highly invasive spheroids that possess elevated cell surface EGFR levels

We next utilized normal murine mammary gland (NMuMG) cells to more appropriately address the hypothesis that EMT stimulated by TGF-β was sufficient to engender MECs with the ability to invade in response to EGF (Miettinen *et al.*, 1994). Figure 2a shows that NMuMG cells endogenously expressed moderate levels of EGFR, which were readily activated along with ERK1/2 in response to EGF (Figure *2a*). We demonstrated the specificity of these responses to stimulation by EGF by treating the cells with *(i)* the Src inhibitor PP2, which uncoupled EGF from phosphorylating EGFR on Y845, but was without effect on EGFR autophosphorylation (*i.e.*, Y1116) and ERK1/2 activation; and *(ii)* the EGFR inhibitor AG1478 (AG), which prevented all three EGF-driven responses (Figure 2*a*). However, despite their expression of functional EGFR, NMuMG cells did not invade to EGF prior to their induction of EMT by TGF-β, which conferred robust invasive activities in response to EGF (Figure 2*b*). Consistent with what we observed in 4T07 cells, post-EMT NMuMG cells displayed an “invasosphere” morphology when cultured on Matrigel (Figure *2b*). Moreover, NMuMG cells only displayed a proliferative response to EGF subsequent to their induction of EMT (Figure 2*c*). However, the growth of pre- and post-EMT NMuMG cell populations remained sensitive to the cytostatic activities of TGF-β (Figure 2*c*).

We next found that TGF-β stimulation of EMT increased the expression of EGFR proteins, a response that was maximal at 4 h and was maintained throughout the 48 h EMT process (Figure *2d*). This response was independent of a change in EGFR mRNA (Figure *2e*), but was dependent on the activity of Src (Figure *2f*). Finally, whole cell EGF binding assays suggested that TGF-β-induced EMT stabilized EGFR on the cell surface (Figure *2g*). Taken together, these findings suggest that the induction of EMT by TGF-β increases stability of

Author Manuscript Author Manuscript Author Manuscript Author Manuscript

EGFR at the cell surface in transitioning cells, which imparts post-EMT MECs with invasive functions in response to EGF.

EMT increases the coupling of EGFR to p38 MAPK activation *via* FAK

We next sought to determine the function of FAK in regulating EGF signaling in post-EMT MECs. As shown in Figure *3a*, EGF-mediated activation p38 MAPK and Src-dependent phosphorylation of EGFR at Y845 were greatly augmented in post-EMT NMuMG cells. Importantly, both of these post-EMT EGF signaling events were completely blocked in NMuMG cells depleted in FAK expression (Figure *3a*). Recent findings suggest that TGF-β transactivates the EGFR pathway *via* an extracellular mechanism involving the protease TACE, whose activation by TGF-β mediates the release of EGF ligands (Wang *et al.*, 2008; Wang *et al.*, 2009). Supplemental Figure 3 shows that pharmacological antagonism of TACE or EGFR had no effect on TGF-shows that pharmacological antagonism of-mediated p38 MAPK activation. Furthermore, Figure *3b* shows that constitutively elevating EGFR expression in NMuMG cells failed to affect the coupling of TGF-shows that pharmacological antagonism of to p38 MAPK. Interestingly, this same cellular condition specifically enhanced the coupling of EGF to p38 MAPK, but had no affect on the extent of ERK1/2 phosphorylation induced by EGF (Figure. *3b*). Taken together, these findings suggest that the activation of p38 MAPK by TGF-β takes place *via* a FAK:Src pathway, whose activation by TGF-b stabilizes EGFR cell surface expression and enables its coupling to p38 MAPK.

In further addressing the function of FAK in mediating the ability of EGF to induce the invasion of post-EMT MECs, we observed that NMuMGs depleted in FAK expression fail to undergo invasion to EGF in the post-EMT state (Figure *3c*). Furthermore, a pharmacological inhibitor of FAK, PF-562271 (PF-271) (Roberts *et al.*, 2008) similarly abrogated the invasion of post-EMT control (*i.e.* YFP) NMuMG cells (Figure *3d*). Along these lines, inclusion of small molecule inhibitors against TbR-I (*i.e.*, SB431542), p38 MAPK (*i.e.*, SB203580), or EGFR (*i.e.*, AG1478) also significantly inhibited the invasion of post-EMT control (*i.e.* YFP) NMuMG cells to EGF (Figure. *3d*). Finally, in light of the elevated expression of EGFR in post-EMT NMuMG cells (Figure *2*), we repeated these pharmacological analyses in EGFR-expressing NMuMG cells. Figure 3e shows that constitutive EGFR expression was sufficient to induce invasion to EGF, a cellular reaction that was drastically potentiated in the post-EMT state. As above, pharmacological inhibition of FAK abrogated pre- and post-EMT invasion of EGFR-expressing NMuMG cells to EGF (Figure. 3e). In stark contrast to their control (*i.e.* YFP) counterparts (Figure. *3d*), treating post-EMT EGFR-expressing NMuMG cells with inhibitors against either TβR-I or p38 MAPK failed to affect invasion elicited by EGF (Figure *3e*). Taken together, these findings suggest that elevated EGFR expression that typically occurs in metastatic breast cancers (Tischkowitz *et al.*, 2007) is sufficient in *(i)* stabilizing the EMT phenotype, *(ii)* allowing persistent invasion to EGF, and *(iii)* conferring resistance to small molecules inhibitors against TβR-I and p38 MAPK.

Author Manuscript Author Manuscript Author Manuscript Author Manuscript

EGFR overexpression transforms NMuMG cells and sensitizes them to EMT by altering EGFR complexes

Given the profound impact constitutive EGFR expression had on EMT-induced invasion to EGF, we next sought to utilize this NMuMG cell model to further characterize the potential role of EMT in facilitating the ability of EGF to induce breast cancer invasion and metastasis. In doing so, we observed constitutive EGFR expression to be sufficient in transforming NMuMG cells, enabling their production of mammary fat pad tumors that were comparable to those formed by NMuMG cells engineered to express polyoma middle T (PyMT; Figure *4a*). Interestingly, the expression of PyMT in NMuMG cells induced a mesenchymal morphology consistent with increased levels of EGFR and its binding of EGF [Supplemental Figure 4; (Salomon *et al.*, 1987)]. Along these lines, constitutive EGFR expression greatly enhanced the mesenchymal character of NMuMG cells stimulated by either TGF-β, EGF, or both cytokines together (Figures *4b*, *4c*).

Given our findings that suggested that diminished E-cadherin expression determines breast cancer invasion to EGF (Figure 1), we next sought to identify the affects of TGF-β on the physical interaction between EGFR and E-cadherin (Bremm *et al.*, 2008; Wilding *et al.*, 1996). Figure *4d* shows that short-term TGF-β stimulation was unable to affect the expression of E-cadherin or EGFR in confluent cultures (*bottom panel*). However, we did observe TGF-β to disband the tonic interaction between EGFR and E-cadherin in favor of forming of EGFR:TbR-II signaling complexes. Moreover, constitutive EGFR expression alone was sufficient in eliciting a stronger interaction between EGFR and TβR-II that mirrored the disassociation of E-cadherin from EGFR, an effect that was further exacerbated by TGF-β treatment (Figure *4d*). Importantly, the formation of TβR-II:EGFR complexes correlated with increased Smad2/3 transcriptional activity and maintained cytostatic response to TGF-β (Supplemental Figure 5). To further explore the relationship between EGFR and E-cadherin, we performed immunofluorescent analyses to monitor changes in their expression and localization in NMuMG cells before and after TGF-β-stimulated EMT. E-cadherin expression was indeed decreased and delocalized from cell-cell junctions in EGFR-expressing NMuMG cells as compared to their control counterparts, findings that were exacerbated upon TGF-β stimulation (Figure 5*a*). Along these lines, Figure *5b* clearly shows an emergence of $EGFR^{high}$/$E\text{-cadherin}^{low}$ post-EMT NMuMG cells. Moreover, the most morphologically “mesenchymal” MECs were completely devoid of both E-cadherin and EGFR expression (Figure *5b* & Supplemental Figure *6*). Taken together, our findings point to the emergence of a post-EMT breast cancer cell population that is E-cadherin-negative, EGFR-positive, and poised to exhibit hyper-invasive responses to EGF.

MEC branching induced by EGFR is dependent upon TGF-β:FAK signaling

We next sought to evaluate the effects of EMT and constitutive EGFR expression on the growth and morphology of MECs propagated in 3D-organotypic systems. As we noted previously (Wendt *et al.*, 2009b), NMuMG cells readily formed organized and hollow acinar structures with a defined actin cytoskeleton when grown in 3D-organotypic conditions (Figure 6*a*). In stark contrast, and reminiscent of what we observed for nonmetastatic breast cancer cells (Figure 1*a*), EGFR-expressing NMuMG cells were found to form multicellular and highly branched 3D structures (30.18%, ± 6.51 of structures were branched; Figure *6a*).

Author Manuscript Author Manuscript Author Manuscript Author Manuscript

These branched organoids may represent an exaggerated activation of normal mammary gland branching activities, particularly since EGF stimulation of parental NMuMG cells also generated branched structures that displayed a more differentiated phenotype (48.75 ± 4.71% of structures were branched; Figure *6b* and 7*b*). Pharmacological inactivation of either TGF-β or EGFR signaling completely abrogated mammary branching (0% of structures were branched) and was sufficient in restoring normal, hollow acinar development by EGFR-expressing NMuMG cells (Figure *6b*). Chemotherapeutic targeting of FAK (PF-271) prevented mammary branching (0% of structures were branched) and acinar hollowing (0% of structures were hollowed; Figure *6b*). Finally, while 3D cultures of post-EMT NMuMG cells failed to elicit any branching structures, this system did produce a significant reduction in acinar hollowing (Figure *6c*). Collectively, these findings suggest that the selective appearance of these post-EMT cellular aggregates likely represent the hyper-invasive spheroids characteristic of metastatic MECs.

EMT prevents EGF-induced mammary branching and enhances pulmonary tumor growth

We next aimed to determine which 3D morphology (*i.e*., branching or aggregate spheroid) was dominant under EGF-stimulated conditions. Thus, pre- and post-EMT control (*i.e.*, YFP) and EGFR-expressing NMuMG cells were propagated in 3D cultures, supplemented with EGF or the EGFR inhibitor, AG1478. As observed above (Figure *6b*), EGF stimulation of control and EGFR-expressing NMuMG cells readily promoted the formation of normal and dysmorphic branching structures, respectively (Figure *7a*). More importantly, Figure 7b and 7c show that TGF-β stimulation of EMT severely blunted the ability of EGF and EGFR to promote organoid branching, and instead induced the appearance of large, dense cellular aggregates characteristic of metastatic MECs (Figure *1a*). Indeed, induction of EMT enhanced pulmonary tumor growth and decreased the survival rate of mice injected with EGFR-transformed NMuMG cells (Figures *7d* and *7e*).

DISCUSSION

The increased ability of TGF-β to induce EMT supports the conversion of TGF-β from restraining tumor formation to encouraging their dissemination to distant secondary sites (Tian and Schiemann, 2009; Wendt *et al.*, 2009a). Although TGF-β and EGF ligands have a long standing pathophysiological association with one another, surprisingly little is known about how these signaling systems cross-talk with one another to impact metastasis. Whereas previous reports suggest that TGF-β transactivates EGFR by liberation of EGF ligands (Thomson *et al.*, 2008; Wang *et al.*, 2008; Wang *et al.*, 2009), we now show for the first time that TGF-β stimulation of EMT elicits a fundamental change in the coupling of EGFR to its downstream effectors. Furthermore, we show that in 3D-organotypic-culture post-EMT MECs manifest as dense cellular aggregates that are characteristic of highly metastatic breast cancer cells. Most importantly, we provide evidence that a two-pronged chemotherapeutic approach that targets FAK in conjunction with EGFR specifically inhibited the oncogenic activities of EGF in these aggressive, post-EMT spheroids.

A key regulatory step during EMT is the loss of E-cadherin expression and activity (Thiery *et al.*, 2009; Wendt *et al.*, 2009a; Yang and Weinberg, 2008). We observed EMT induced by

Author Manuscript Author Manuscript Author Manuscript Author Manuscript

TGF-β to not only downregulate E-cadherin expression, but also to prevent its interaction with EGFR, allowing for the formation of EGFR:TβR-II complexes that stabilized EGFR at the cell surface of post-EMT MECs. Along these lines, TGF-β has recently been shown to diminish autocrine EGF ligand production (Thomson *et al.*, 2008). Indeed, under these conditions we show that EGFR exhibits heightened availability and responsiveness to paracrine EGF, a signal initiated *in vivo* by reactive tumor stroma (Wyckoff *et al.*, 2004). Accordingly, we observed elevated EGFR expression to effectively transform NMuMG cells, as well as to induce their delocalization and downregulation of E-cadherin expression.

While the overall levels of EGFR were consistently upregulated in parental NMuMG cells undergoing EMT stimulated by TGF-β, we did identify another highly "mesenchymal-type" population of post-EMT NMuMG cells that lacked EGFR expression. Indeed, a recent study found that prolonged EMT induced by TGF-β (21 days) could elicit cellular switching of receptor tyrosine kinases from a predominantly EGFR-dependent phenotype to one that is dependent upon the receptors for FGF or PDGF (Thomson *et al.*, 2008). Whether a similar "switching" mechanism is transpiring in these highly mesenchymal and EGFR-deficient MECs remains to be determined definitively. However, using isogenic cell lines derived from nonmetastatic 67NR cells, we do show for the first time that highly mesenchymal appearing cells cultured on plastic manifest as dense cellular spheroids under 3D culture conditions. Indeed, our findings may offer a novel explanation as to why science and medicine routinely fail to identify EMT in human tumors, particularly in metastatic tumor tissue growing in compliant environments like the lungs. Should this prove to be a universal phenomenon, it stands to reason that determining the molecular mechanisms whereby these novel "invasospheres" undergo invasion seems particularly meritus. In fact, our preliminary analyses suggest that "invasospheres" can traverse synthetic basement membranes as a single, cooperating unit (*data not shown*), which contrasts sharply with the initiation of single cell-based programs of mesenchymal or amoeboid invasion (Friedl and Brocker, 2000).

In addition to our identification of a unique mode of MEC invasion, our *in vitro* protocol of first eliciting EMT in MECs, followed by their subsequent dissociation and subculture in 3D-organotypic systems in many respects recapitulates the steps of breast cancer cell metastasis – *i.e.*, primary carcinoma cells undergo EMT, exit the primary tumor, survive anoikis in the circulation, and finally invade and grow out in a new compliant microenvironment, such as the lung. Indeed, the propagation of breast cancer cells in 3D cultures has been proposed as a model that strongly recapitulates the outgrowth of breast cancer cells in the lung (Shibue and Weinberg, 2009). As depicted in Figure *7e*, we propose that breast cancer cells that have undergone EMT abandon their inherent branching program to instead acquire an "invasosphere" morphology that enables these structures to form large, undifferentiated metastases at distant locales. This model is further supported by our data showing that induction of EMT not only increases primary tumor exit, but also enhances the outgrowth of pulmonary tumors established by tail vein injection.

In attempting to translate our findings to the clinic, it remains to be determined whether the recent inclusion of elevated EGFR expression to the basal-like/triple-negative gene signatures is indicative of the stabilized EGFR phenotype we observed in post-EMT MECs

Author Manuscript Author Manuscript Author Manuscript Author Manuscript

(Tischkowitz *et al.*, 2007). However, EMT stimulated by TGF-β does result in the expression of Snail, which subsequently promotes the downregulation of estrogen receptor-α (Dhasarathy *et al.*, 2007). Thus, our findings wholly support a model whereby distinct subpopulations of breast cancer cells undergo EMT, thereby contributing to the development of a gene signature that is indicative of poor clinical outcomes. More importantly, our findings indicate that chemotherapeutic targeting of the TGF-β signaling system that results in its pan-antagonism may offer little-to-no therapeutic benefit in post-EMT MECs that exhibit elevated EGFR expression. Moreover, our analyses also suggest that simultaneous targeting of FAK in conjunction with EGFR, may provide a highly effective means to inhibit these hyper-invasive, post-EMT "invasospheres." Experiments designed to test this clinically relevant hypothesis are currently ongoing.

MATERIALS AND METHODS

Cell lines and retroviral reagents

Normal murine mammary gland (NMuMG) cells were obtained from ATCC (Manassas, VA, USA) and cultured as described previously (Galliher and Schiemann, 2007), as was the construction of NMuMG cells that lacked FAK expression (Wendt and Schiemann, 2009). NMuMG cells were engineered to express elevated levels of EGFR by their transduction with VSVG retroviral particles that encoded for either *YFP* or *EGFR* (*i.e.*, pBabe-*YFP* or pBabe-*EGFR*, respectively, and provided by Dr. Alexander Sorkin (University of Pittsburg, Pittsburg, PA). Afterward, polyclonal populations of transduced NMuMG cells were isolated by puromycin selection (5 μg/ml) for 14 days. In addition, NMuMG cells were also transduced with murine ecotropic viral particles that encoded for either *GFP* or *PyMT* (*i.e.*, pMSCV-IRES-*GFP* or pMIG-*PyMT*-IRES-*GFP*, respectively), and transduced NMuMG cells expressing GFP were isolated by flow-cytometry as described previously (Galliher and Schiemann, 2007). The human MCF10A cell derivates T1k and Ca1h were cultured as described previously (Wendt and Schiemann, 2009), as were the conditions necessary to propagate the human MCF-7 (Micalizzi *et al.*, 2009), MDA-MB-231 (Wendt *et al.*, 2008), 4T1, 4T07 and 67NR (Wendt *et al.*, 2009b) cells. Throughout the study, we refer to post-EMT NMuMG cells as those that were stimulated on plastic for 48 h with TGF-β1 (5 ng/ml), while post-EMT 4T07 cells were obtained following three weeks of continuous TGF-β stimulation through several passages. In all cases pre-EMT cells represent their unstimulated counterparts.

Cell signaling, immunoblotting, and immunoprecipitation assays

To monitor the activation status of TGF-β and EGF effectors, pre-EMT and post-EMT MECs were serum-deprived (0.5% FBS) for 6 h prior to their stimulation with TGF-β1 (5 ng/ml) or EGF (50 ng/ml) for varying times as indicated. Afterward, clarified whole-cell extracts were prepared as described previously (Wendt and Schiemann, 2009; Wendt *et al.*, 2009b) and subjected to immunoblot analyses using the primary antibodies listed in the supplementary materials.

In some experiments, confluent cultures of control (*i.e.*, YFP) or EGFR-expressing NMuMG cells were treated for 24 h with TGF-β1 (5 ng/ml) prior to isolating EGFR complexes using

Author Manuscript Author Manuscript Author Manuscript Author Manuscript

previously described immunoprecipitation conditions (Galliher and Schiemann, 2006). The resulting EGFR immunocomplexes (anti-EGFR antibodies: 1:100, Cell Signaling) were immunoblotted with antibodies against TβR-II, FAK, E-cadherin, and β-actin as described above.

Cell biological assays

The inhibition of DNA synthesis by TGF-β was determined using [^{3}H]thymidine incorporation assays as described previously (Wendt *et al.*, 2009b). To monitor the ability of EGF to induce DNA synthesis, pre- and post-EMT NMuMG cells were subcultured onto 24-well plates (20,000 cells/well) and allowed to adhere for 4 h, at which point the growth-media was removed and replaced with serum-free media supplemented with either TGF-β1 (5 ng/ml), EGF (50 ng/ml), or both cytokines. Twenty-four h later, the cells were treated with [^{3}H]thymidine, whose incorporation into cellular DNA was quantified as described previously (Wendt *et al.*, 2009b).

The ability of EGF (50 ng/ml) or serum (2%) to alter the invasion of pre- or post-EMT cells was analyzed using a modified Boyden Chamber assay (50,000 cells/well) as described previously (Wendt and Schiemann, 2009), where all values are normalized to a serum-free control set to 100%. In some experiments, the following pharmacological inhibitors were included with EGF throughout the assay: *a)* the TβR-I inhibitor, SB431542 (10 μg/ml; EMD Biosciences, San Diego, CA); *b)* the FAK inhibitor, PF562271 (1 μM; Pfizer Inc., Groton, CT); *c)* the p38 MAPK, SB230580 (10 μM; EMD Biosciences); or *d)* the EGFR inhibitor, AG1478 (1 μM; Cayman Chemical, Ann Arbor, MI).

The ability of TGF-β1 (5 ng/ml), EGF (50 ng/ml), or both cytokines to alter the actin cytoskeleton in NMuMG cells was visualized using TRITC-conjugated phalloidin (0.25 μM; Invitrogen) as described previously (Galliher and Schiemann, 2006). In some experiments, alterations in the expression and/or localization of E-cadherin and EGFR was monitored by indirect immunofluorescence where the cells were *(i)* fixed in 4% paraformaldehyde; *(ii)* permeablized in 0.1% Triton X-100; and *(iii)* stained with anti-E-cadherin (1:250) or EGFR (1:100) antibodies. Afterward, E-cadherin immunocomplexes were visualized using biotinconjugated goat anti-mouse antibodies (Jackson ImmunoResearch, West Grove, PA) in combination with Texas-Red-labeled avidin (Vector Laboratories, Burlingame, CA), while EGFR immunocomplexes were visualized simultaneously using FITC-labeled donkey anti-rabbit secondary antibodies (Jackson ImmunoResearch, West Grove, PA, USA).

EGFR expression analyses

We also monitored alterations in EGFR expression using real-time PCR as described in the supplementary methods. In addition, pre- and post-EMT NMuMG (1×10^6) cells were resuspended in enzyme-free cell disassociation buffer (Invitrogen, Carlsbad, CA), and subsequently incubated in PBS supplemented with 0.1% BSA, to which diluent or Alexa488-labled EGF (50 ng/ml; Invitrogen) was added. The cells were labeled in the dark and on ice for 45 min, at which point they were washed extensively with ice-cold PBS, fixed in 1% paraformaldehyde, and analyzed by flow-cytometry.

Author Manuscript Author Manuscript Author Manuscript Author Manuscript

Tumor growth analyses

Control (*i.e.*, YFP), PyMT-, and EGFR-expressing NMuMG (2×10^6) cells were resuspended in sterile PBS (50 μl) that contained 5% Matrigel (BD Biosciences), and subsequently injected into the mammary fat-pad of 6 week old female Nu/Nu mice (Charles River, Wilmington, MA). Tumor growth was assessed by calculating primary tumor volumes using digital calipers and the following equation: Tumor Volume = $(x^2)(y)(0.5)$, where x is the tumor width and y is tumor length. Alternatively, pre- and post-EMT NmuMG-EGFR (4×10^5) cells were injected into the lateral tail vein of female Nu/Nu mice and pulmonary tumor growth was monitored by bioluminecent analysis using the Xenogen IVIS200 imager as described previously (Wendt and Schiemann, 2009). Luciferase expressing 4T1 (1×10^4), 4T07 (1×10^5) or 67NR (1×10^5) cell were resuspended in sterile PBS (50 μl) and engrafted onto the mammary fat pad of 6 week old female Balb/C mice and pulmonary metastasis was monitored as above. All animal studies were performed according to animal protocol procedures approved by the Institutional Animal Care and Use Committee of the University of Colorado.

3-Dimensional (3D)-organotypic assays

Pre- and post-EMT NMuMG or 4T07 (1×10^4) cells were resuspended in growth media supplemented with 5% Cultrex (R&D Systems, Minneapolis, MN), and subsequently seeded in 48-well plates onto Cultrex cushions (150 μl/well). In some experiments, acinar development was allowed to transpire in the continued presence of EGF (50 ng/ml), SB431542 (10 μg/ml), PF562271 (1 μM), or AG1478 (1 μM) as indicated. All NMuMG 3D-organotypic cultures were fed on day 7 and were allowed to develop for an additional 3 days, at which point the extent of their hollowing and branching was assessed by phase-contrast microscopy and quantified by three individuals who were blinded to the culture conditions. Where indicated, acinar development also transpired on 8-well chamber slides, which were processed on day 10 for TRITC-conjugated phalloidin (0.25 μM; Invitrogen) and DAPI staining as described above. All 4T1, 4T07, and 67NR 3D-organotypic cultures were grown for 5 days and similarly assayed for branching as described above.

Statistical analyses

Statistical values were defined using an unpaired student's T-test, where a P value < 0.05 was considered significant. P values for all experiments analyzed are indicated.

Supplementary Material

Refer to Web version on PubMed Central for supplementary material.

ACKNOWLEDGEMENTS

We thank Pfizer for graciously providing the novel small molecule FAK inhibitor, PF-562271. We also thank Dr. Alexander D. Sorkin for providing the retroviral construct that encoded human EGFR. W.P.S. was supported in part by grants from the National Institutes of Health (CA129359) and the Susan G. Komen for the Cure Foundation (BCTR0706967) and the Department of Defense (BC084561), while M.K.W. was supported by a fellowship from the American Cancer Society (PF-09-120-01).

Author Manuscript Author Manuscript Author Manuscript Author Manuscript

Research support: was provided in part by the National Institutes of Health (CA129359), the Komen Foundation (BCTR0706967), and the Department of Defense (BC084561) to W.P.S., and by the American Cancer Society (PF-09-120-01) to M.K.W.

REFERENCES

Aslakson CJ, Miller FR. Selective events in the metastatic process defined by analysis of the sequential dissemination of subpopulations of a mouse mammary tumor. Cancer Res. 1992; 52:1399–1405. [PubMed: 1540948]

Barr S, Thomson S, Buck E, Russo S, Petti F, Sujka-Kwok I, et al. Bypassing cellular EGF receptor dependence through epithelial-to-mesenchymal-like transitions. Clin Exp Metastasis. 2008; 25:685–693. [PubMed: 18236164]

Bremm A, Walch A, Fuchs M, Mages J, Duyster J, Keller G, et al. Enhanced activation of epidermal growth factor receptor caused by tumor-derived E-cadherin mutations. Cancer Res. 2008; 68:707–714. [PubMed: 18245470]

Buck E, Eyzaguirre A, Barr S, Thompson S, Sennello R, Young D, et al. Loss of homotypic cell adhesion by epithelial-mesenchymal transition or mutation limits sensitivity to epidermal growth factor receptor inhibition. Mol Cancer Ther. 2007; 6:532–541. [PubMed: 17308052]

Park MB CC, Barcellos-Hoff MH. The influence of the microenvironment on the malignant phenotype. Mol Med Today. 2000; 6:324–329. [PubMed: 10904250]

Cicchini C, Laudadio I, Citarella F, Corazzari M, Steindler C, Conigliaro A, et al. TGF-β-induced EMT requires focal adhesion kinase (FAK) signaling. Exp Cell Res. 2008; 314:143–152. [PubMed: 17949712]

Cowin P, Welch DR. Breast cancer progression: controversies and consensus in the molecular mechanisms of metastasis and EMT. J Mammary Gland Biol Neoplasia. 2007; 12:99–102. [PubMed: 18769505]

DeNardo DG, Barreto JB, Andreu P, Vasquez L, Tawfik D, Kolhatkar N, et al. CD4(+) T cells regulate pulmonary metastasis of mammary carcinomas by enhancing protumor properties of macrophages. Cancer Cell. 2009; 16:91–102. [PubMed: 19647220]

Dhasarathy A, Kajita M, Wade PA. The transcription factor Snail mediates epithelial to mesenchymal transitions by repression of estrogen receptor α. Mol Endocrinol. 2007; 21:2907–2918. [PubMed: 17761946]

Ding Q, Gladson CL, Wu H, Hayasaka H, Olman MA. FAK-related non-kinase inhibits myofibroblast differentiation through differential MAPK activation in a FAK-dependent manner. J Biol Chem. 2008; 283:26839–26849. [PubMed: 18669633]

Friedl P, Brocker EB. The biology of cell locomotion within three-dimensional extracellular matrix. Cell Mol Life Sci. 2000; 57:41–64. [PubMed: 10949580]

Galliher AJ, Schiemann WP. β3 integrin and Src facilitate TGF-β mediated induction of epithelial-mesenchymal transition in mammary epithelial cells. Breast Cancer Res. 2006; 8:R42. [PubMed: 16859511]

Galliher AJ, Schiemann WP. Src phosphorylates Tyr284 in TGF-β type II receptor and regulates TGF-β stimulation of p38 MAPK during breast cancer cell proliferation and invasion. Cancer Res. 2007; 67:3752–3758. [PubMed: 17440088]

Hugo H, Ackland ML, Blick T, Lawrence MG, Clements JA, Williams ED, et al. Epithelial--mesenchymal and mesenchymal--epithelial transitions in carcinoma progression. J Cell Physiol. 2007; 213:374–383. [PubMed: 17680632]

Joo CK, Kim HS, Park JY, Seomun Y, Son MJ, Kim JT. Ligand release-independent transactivation of epidermal growth factor receptor by TGF-β involves multiple signaling pathways. Oncogene. 2007; 27:614–628. [PubMed: 17637750]

Kalluri R, Weinberg RA. The basics of epithelial-mesenchymal transition. J Clin Invest. 2009; 119:1420–1428. [PubMed: 19487818]

Kenny PA, Lee GY, Myers CA, Neve RM, Semeiks JR, Spellman PT, et al. The morphologies of breast cancer cell lines in three-dimensional assays correlate with their profiles of gene expression. Mol Oncol. 2007; 1:84–96. [PubMed: 18516279]

Author Manuscript Author Manuscript Author Manuscript Author Manuscript

Micalizzi DS, Christensen KL, Jedlicka P, Coletta RD, Baron AE, Harrell JC, et al. The Six1 homeoprotein induces human mammary carcinoma cells to undergo epithelial-mesenchymal transition and metastasis in mice through increasing TGF-β signaling. J Clin Invest. 2009; 119:2678–2690. [PubMed: 19726885]

Miettinen PJ, Ebner R, Lopez AR, Derynck R. TGF-β induced transdifferentiation of mammary epithelial cells to mesenchymal cells: involvement of type I receptors. J Cell Biol. 1994; 127:2021–2036. [PubMed: 7806579]

Mitra SK, Lim ST, Chi A, Schlaepfer DD. Intrinsic focal adhesion kinase activity controls orthotopic breast carcinoma metastasis via the regulation of urokinase plasminogen activator expression in a syngeneic tumor model. Oncogene. 2006; 25:4429–4440. [PubMed: 16547501]

Moustakas A, Heldin CH. Signaling networks guiding epithelial-mesenchymal transitions during embryogenesis and cancer progression. Cancer Sci. 2007; 98:1512–1520. [PubMed: 17645776]

Padua D, Zhang XH, Wang Q, Nadal C, Gerald WL, Gomis RR, et al. TGF-β primes breast tumors for lung metastasis seeding through angiopoietin-like 4. Cell. 2008; 133:66–77. [PubMed: 18394990]

Perou CM, Sorlie T, Eisen MB, van de Rijn M, Jeffrey SS, Rees CA, et al. Molecular portraits of human breast tumours. Nature. 2000; 406:747–752. [PubMed: 10963602]

Roberts WG, Ung E, Whalen P, Cooper B, Hulford C, Autry C, et al. Antitumor activity and pharmacology of a selective focal adhesion kinase inhibitor, PF-562,271. Cancer Res. 2008; 68:1935–1944. [PubMed: 18339875]

Saha D, Datta PK, Sheng H, Morrow JD, Wada M, Moses HL, et al. Synergistic induction of cyclooxygenase-2 by TGF-β1 and epidermal growth factor inhibits apoptosis in epithelial cells. Neoplasia. 1999; 1:508–517. [PubMed: 10935498]

Salomon DS, Perroteau I, Kidwell WR, Tam J, Derynck R. Loss of growth responsiveness to epidermal growth factor and enhanced production of α-transforming growth factors in Ras-transformed mouse mammary epithelial cells. J Cell Physiol. 1987; 130:397–409. [PubMed: 3494020]

Shibue T, Weinberg RA. Integrin b1-focal adhesion kinase signaling directs the proliferation of metastatic cancer cells disseminated in the lungs. Proc Natl Acad Sci U S A. 2009; 106:10290–10295. [PubMed: 19502425]

Sieg DJ, Hauck CR, Ilic D, Klingbeil CK, Schaefer E, Damsky CH, et al. FAK integrates growth-factor and integrin signals to promote cell migration. Nat Cell Biol. 2000; 2:249–256. [PubMed: 10806474]

Sorlie T, Perou CM, Tibshirani R, Aas T, Geisler S, Johnsen H, et al. Gene expression patterns of breast carcinomas distinguish tumor subclasses with clinical implications. Proc Natl Acad Sci U S A. 2001; 98:10869–10874. [PubMed: 11553815]

Sorlie T, Tibshirani R, Parker J, Hastie T, Marron JS, Nobel A, et al. Repeated observation of breast tumor subtypes in independent gene expression data sets. Proc Natl Acad Sci U S A. 2003; 100:8418–8423. [PubMed: 12829800]

Takahashi K, Suzuki K. Density-dependent inhibition of growth involves prevention of EGF receptor activation by E-cadherin-mediated cell-cell adhesion. Exp Cell Res. 1996; 226:214–222. [PubMed: 8660958]

Tarin D, Thompson EW, Newgreen DF. The fallacy of epithelial mesenchymal transition in neoplasia. Cancer Res. 2005; 65:5996–6000. [PubMed: 16024596]

Thiery JP, Acloque H, Huang RY, Nieto MA. Epithelial-mesenchymal transitions in development and disease. Cell. 2009; 139:871–890. [PubMed: 19945376]

Thomson S, Buck E, Petti F, Griffin G, Brown E, Ramnarine N, et al. Epithelial to mesenchymal transition is a determinant of sensitivity of non-small-cell lung carcinoma cell lines and xenografts to epidermal growth factor receptor inhibition. Cancer Res. 2005; 65:9455–9462. [PubMed: 16230409]

Thomson S, Petti F, Sujka-Kwok I, Epstein D, Haley JD. Kinase switching in mesenchymal-like non-small cell lung cancer lines contributes to EGFR inhibitor resistance through pathway redundancy. Clin Exp Metastasis. 2008; 25:843–854. [PubMed: 18696232]

Tian M, Schiemann WP. The TGF-β paradox in human cancer: an update. Future Oncol. 2009; 5:259–271. [PubMed: 19284383]

Author Manuscript Author Manuscript Author Manuscript Author Manuscript

Tischkowitz M, Brunet J-S, Begin L, Huntsman D, Cheang M, Akslen L, et al. Use of immunohistochemical markers can refine prognosis in triple negative breast cancer. BMC Cancer. 2007; 7:134. [PubMed: 17650314]

Wang SE, Xiang B, Guix M, Olivares MG, Parker J, Chung CH, et al. TGF-β engages TACE and ErbB3 to activate phosphatidylinositol-3 kinase/Akt in ErbB2-overexpressing breast cancer and desensitizes cells to Trastuzumab. Mol Cell Biol. 2008; 28:5605–5620. [PubMed: 18625725]

Wang SE, Xiang B, Zent R, Quaranta V, Pozzi A, Arteaga CL. TGF-β induces clustering of HER2 and integrins by activating Src-focal adhesion kinase and receptor association to the cytoskeleton. Cancer Res. 2009; 69:475–482. [PubMed: 19147560]

Wendt M, Schiemann W. Therapeutic targeting of the focal adhesion complex prevents oncogenic TGF-β signaling and metastasis. Breast Cancer Res. 2009; 11:R68. [PubMed: 19740433]

Wendt MK, Allington TM, Schiemann WP. Mechanisms of the epithelial-mesenchymal transition by TGF-β. Future Oncol. 2009a; 5:1145–1168. [PubMed: 19852727]

Wendt MK, Cooper AN, Dwinell MB. Epigenetic silencing of CXCL12 increases the metastatic potential of mammary carcinoma cells. Oncogene. 2008; 27:1461–1471. [PubMed: 17724466]

Wendt MK, Smith JA, Schiemann WP. p130Cas is required for mammary tumor growth and transforming growth factor-beta (TGF-beta)-mediated metastasis through regulation of Smad2/3 activity. J Biol Chem. 2009b; 284:34145–34156. [PubMed: 19822523]

Wilding J, Vousden KH, Soutter WP, McCrea PD, Del Buono R, Pignatelli M. E-cadherin transfection down-regulates the epidermal growth factor receptor and reverses the invasive phenotype of human papilloma virus-transfected deratinocytes. Cancer Res. 1996; 56:5285–5292. [PubMed: 8912870]

Wyckoff J, Wang W, Lin EY, Wang Y, Pixley F, Stanley ER, et al. A paracrine loop between tumor cells and macrophages is required for tumor cell migration in mammary tumors. Cancer Res. 2004; 64:7022–7029. [PubMed: 15466195]

Wyckoff JB, Segall JE, Condeelis JS. The collection of the motile population of cells from a living tumor. Cancer Res. 2000; 60:5401–5404. [PubMed: 11034079]

Yang J, Weinberg RA. Epithelial-mesenchymal transition: at the crossroads of development and tumor metastasis. Dev Cell. 2008; 14:818–829. [PubMed: 18539112]

Zavadil J, Bottinger EP. TGF-β and epithelial-to-mesenchymal transitions. Oncogene. 2005; 24:5764–5774. [PubMed: 16123809]

Author Manuscript Author Manuscript Author Manuscript Author Manuscript

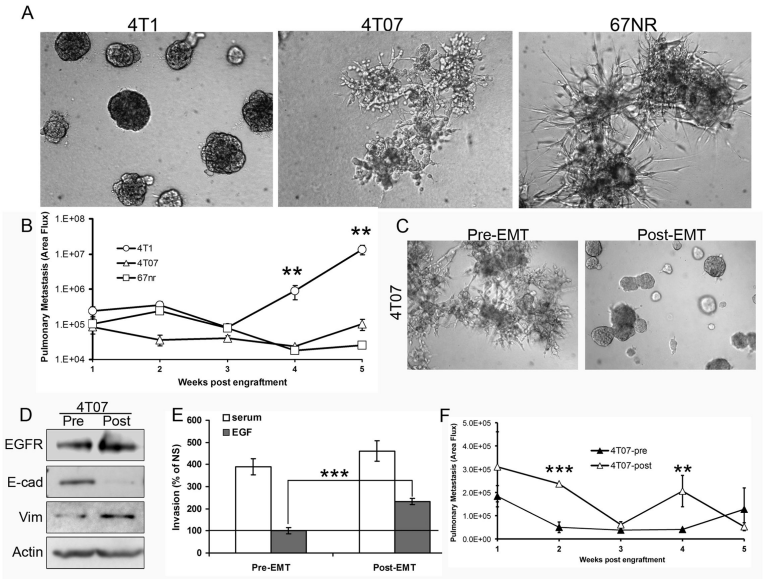

Figure 1.

Loss of mammary branching characterizes increasing metastatic potential and is induced by TGF-β1. *A*) 4T1 (highly metastatic), 4T07 (invasive, but nonmetastatic), and 67NR (noninvasive and nonmetastatic) mammary carcinoma cells were grown in 3D culture for 5 days and representative structures are shown. Data indicate that branching mammary structures are characteristic of non-metastatic cells, a phenotype that is abandon by fully metastatic cells. *B*) The cells described in panel A expressing firefly luciferase were engrafted onto the mammary fat pad of 4 week old female Balb/C mice (4T1=10,000 cells; 4T07 and 67NR= 100,000 cells). Mean pulmonary luminescence (Area flux) is shown at various time points as a measure of metastasis from the primary mammary tumor to the lungs (n=5 mice per group, ±SE,***P*<0.01). *C*) Pre- and post-EMT 4T07 cells were cultured in 3D-organotypic conditions for 5 days and representative structures are shown. *D*) The Pre- and Post-EMT 4T07 cells were analyzed by immunoblot for EGFR, E-cadherin (E-cad), Vimentin (Vim) and β-Actin (Actin) as a loading control. Shown are representative immunoblots that were completed three times with similar results. *E*) Pre- and Post-EMT 4t07 cells were allowed to invade through Matrigel-coated synthetic membranes in response to 2% serum or EGF. Data are normalized to a serum-free control (*solid line at 100%*) and are the mean (±SE) of three independent experiments completed in triplicate (****P*<0.001). *F*) The Pre- and Post-EMT 4T07 cells as in panel C were engrafted onto the mammary fat pad of Balb/C mice as in Panel B. Mean pulmonary luminescence (Area flux) is shown at various time points following engraftment (n=5 mice per group, ±SE, ****P*<0.001, ***P*<0.01).

Author Manuscript Author Manuscript Author Manuscript Author Manuscript

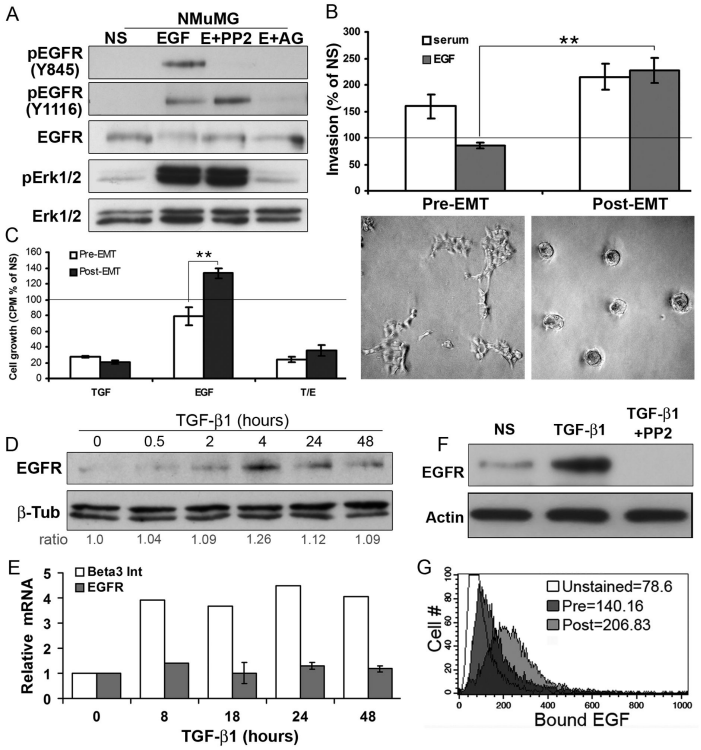

Figure 2.

TGF-β stimulation of EMT results in the generation of highly invasive spheroids that possess elevated EGFR cell surface expression. *A)* NMuMG cells were serum-deprived (0.5% FBS) for 6 h in the absence or presence of the Src inhibitor, PP2 (10μM) or the EGFR inhibitor, AG1478 (1 μM), at which point they were stimulated for 30 min with EGF and analyzed for the phosphorylation of EGFR [pEGFR(Y845)], [pEGFR(Y1116)] or ERK1/2 (pErk1/2). The resulting immunoblots were stripped and reprobed with antibodies against EGFR or ERK1/2, to monitor differences in protein loading. Images are from a representative experiment that was performed at least three times with similar results (NS, no stimulation). *B)* Pre-EMT and post-EMT NMuMG (48 hour pretreatment with TGF-β1 (5ng/ml)) cells were induced to invade synthetic basement membranes by either serum (2%) or EGF (50 ng/ml) as indicated. Data are the mean (± SE) invasion relative to serum free media for both Pre- and Post-EMT cells (*solid line*) observed in three independent experiments completed in triplicate (***P* < 0.01). Accompanying photomicrographs depict the morphology of pre-EMT (*lower left*) and post-EMT (*lower right*) NMuMG cells when propagated for 24 h on Matrigel cushions. *C)* Pre-EMT and post-EMT NMuMG cells were incubated with either TGF-β1 (5 ng/ml), EGF (50 ng/ml), or both cytokines for 24 h prior to labeling cellular DNA by administration of [^{3}H]thymidine. Data are the mean (± SE) quantities of incorporated [^{3}H]thymidine normalized to unstimulated controls (*solid line*) observed in three independent experiments completed in triplicate (***P* < 0.01). *D)* Quiescent NMuMG cells were stimulated with TGF-β1 (5 ng/ml) for indicated times over a period of 48 h, at which point alterations in EGFR expression were monitored by immunoblotting. Stripped membranes were reprobed with anti-β-tubulin (β-Tub) to monitor differences in protein loading. Images are from a representative experiment that was

Author Manuscript Author Manuscript Author Manuscript Author Manuscript

performed at least four times with similar results. *E)* Quiescent NMuMG cells were stimulated with TGF-β1 (5 ng/ml) as in *panel D.* Afterward, total RNA was isolated and subjected to semi-quantitative real-time PCR to monitor the expression of EGFR or β3 integrin, which served as a marker for EMT induced by TGF-β. Data are the mean (±SD) fold changes in gene expression relative to untreated control cells observed in at least three independent experiments. *F)* Quiescent NMuMG cells were stimulated with TGF-β1 (5 ng/ml) for 18 h in the absence or presence the Src inhibitor, PP2 (10 μM). Alterations in EGFR expression were monitored by immunoblotting as in *panel D.G)* Cell surface expression of EGFR in pre-EMT and post-EMT NMuMG cells was determined by flow-cytometric analysis of bound Alexa488-labeled EGF. The presented histogram is representative of three independent experiments.

Author Manuscript Author Manuscript Author Manuscript Author Manuscript

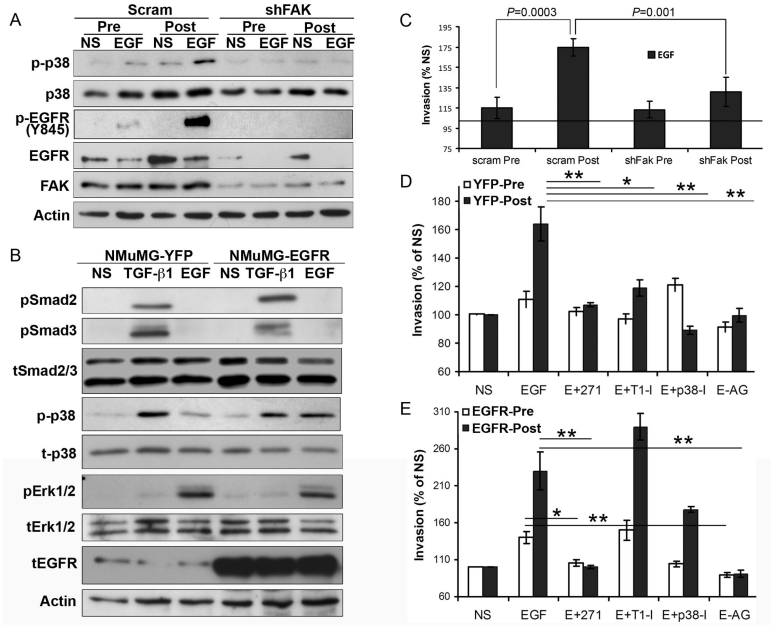

Figure 3.

EMT increases the coupling of EGFR to p38 MAPK activation *via* FAK. *A)* Control (*i.e.*, scrambled shRNA; scram) and FAK-depleted (shFAK) NMuMG cells were incubated in the absence (Pre-EMT) or presence of TGF-β1 (5 ng/ml; Post-EMT) for 48 h, at which point they were washed, serum deprived for 6 h and subsequently stimulated with EGF (50 ng/ml) for 30 min and analyzed for phospho-p38 MAPK (p-p38) or phospho-Y845-EGFR [p-EGFR(Y845)] as indicated. The resulting immunoblots were stripped and reprobed with antibodies against p38 MAPK, EGFR, FAK, and β-actin (Actin) to monitor differences in protein loading. Images are from a representative experiment that was performed four times with similar results (NS, no stimulation). *B)* Quiescent control (*i.e.*, YFP) and EGFR-expressing NMuMG cells were stimulated for 30 min with either TGF-β1 (5 ng/ml) or EGF (50 ng/ml) and analyzed to monitor the phosphorylation status of Smad2 (pSmad2), Smad3 (pSmad3), p38 MAPK (p-p38), and ERK1/2 (pErk1/2). The resulting immunoblots were stripped and reprobed for total Smad2/3 (tSmad2/3), p38 MAPK (t-p38), ERK1/2 (tErk1/2), EGFR and β-actin (Actin) as loading controls. Images are from a representative experiment that was performed at least four times with similar results. *C)* Control (*i.e.*, scrambled shRNA; scram) and FAK-depleted pre- and post-EMT NMuMG cells were allowed to invade synthetic basement membranes in response to EGF (50 ng/ml). Data are the mean (± SE) invasion relative to unstimulated MECs (*i.e.* serum-free media placed in the bottom chamber = solid line *set to 100%*) observed in three independent experiments completed in triplicate. *D)* Pre- and post-EMT control (*i.e.*, YFP) NMuMG cells were induced to invade to EGF (50 ng/ml) in the absence or presence of the following pharmacological inhibitors a FAK inhibitor, PF-562271 (271, 1 μM), TβR-I inhibitor, SB431542 (T1-I, 10 μg/ml), p38 MAPK inhibitor, SB203580 (p38-I, 10 μM), EGFR inhibitor, AG1478 (AG, 1 μM). *E*) Data consists of the identical invasion experiments as in *panelD* completed with the EGFR-expressing (EGFR) NMuMG cells. Presented data in panels D and E are the mean (±SE) invasion relative to an EGF free control (*i.e.* serum free media placed in the bottom chamber

= NS, set to 100%) observed in three independent experiments completed in triplicate. (*P<0.05; **P<0.01).

Author Manuscript Author Manuscript Author Manuscript Author Manuscript

Author Manuscript Author Manuscript Author Manuscript Author Manuscript

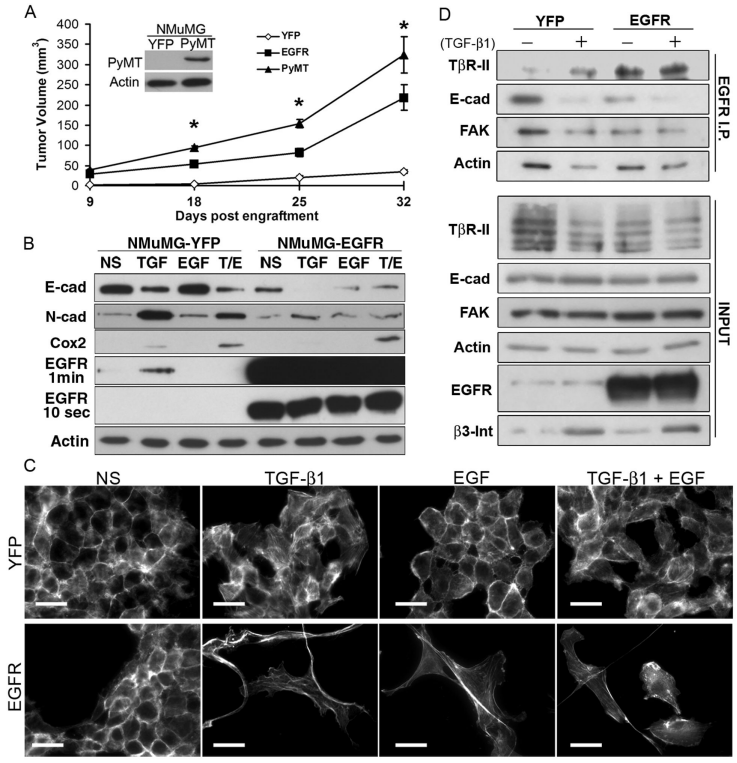

Figure 4.

EGFR overexpression transforms NMuMG cells and sensitizes them to EMT by altering EGFR complexes. *A)* Control (*i.e.*, YFP), PyMT-, and EGFR-expressing NMuMG cells were engrafted onto the mammary fat pads of Nu/Nu mice, whose development of mammary tumors was monitored over 32 days. Data are the mean (± SE) tumor volumes measured for indicated NMuMG tumor variants. (**P*<0.05, n=6 mice/group). Inset depicts PyMT expression in NMuMG cells, which served as a positive control for tumor formation. *B)* Control (*i.e.*, YFP) and EGFR-expressing NMuMG cells were stimulated with TGF-β1 (5 ng/ml), EGF (50 ng/ml), or both cytokines for 48 h as indicated. Afterward, detergent-solubilized whole-cell extracts were prepared and subjected to immunoblot analyses to monitor changes in the expression of E-cadherin (E-cad), N-cadherin (N-cad), cycloxygenase-2 (Cox2), EGFR, and β-actin (Actin), which served as a loading control. Images are from a representative experiment that was performed at least three times in its entirety with similar results. *C)* Control (*i.e.*, YFP) and EGFR-expressing NMuMG cells were stimulated as described in *panelB* prior to visualizing alterations in the actin cytoskeleton by direct phalloidin fluorescence. Images are representative photomicrographs (600x) from a single experiment that was performed two times with identical results. *D)* Control (*i.e.*, YFP) and EGFR-expressing NMuMG cells were allowed to reach confluence to normalize E-cad expression levels and incubated in the absence or presence of TGF-β1 (5 ng/ml) for 24 h prior to isolating EGFR complexes by immunoprecipitation. The resulting EGFR immunocomplexes (EGFR I.P.) were immunoblotted with antibodies against TβR-II, E-cadherin (E-cad), FAK, and β-actin (Actin; *top panel*). Aliquots of the original whole-cell extract (*input*) was also immunoblotted with antibodies against TβR-II, E-cadherin (E-cad), FAK, β-actin (Actin), EGFR, and β3 integrin to control for differences in protein loading

(*bottom panel*). Images are from a representative experiment that was performed three times with similar results.

Author Manuscript Author Manuscript Author Manuscript Author Manuscript

Author Manuscript Author Manuscript Author Manuscript Author Manuscript

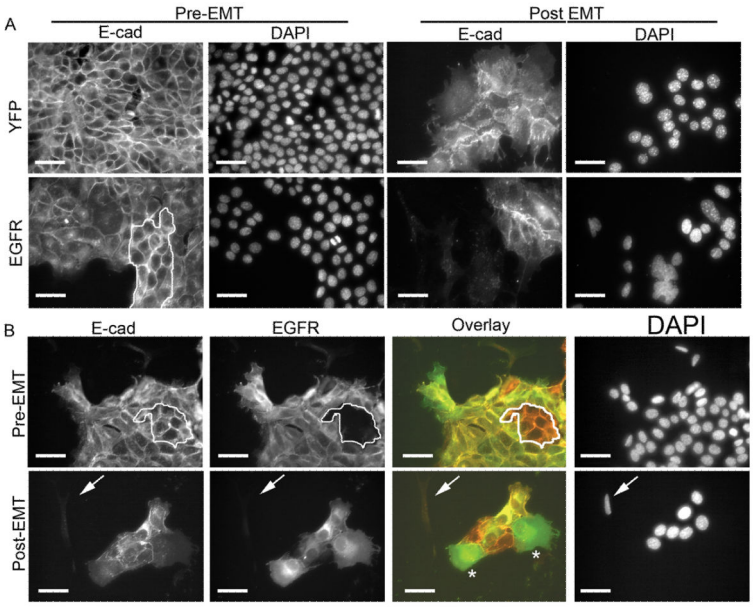

Figure 5.

EGFR expression enhanced the delocalization of E-cadherin induced by EMT. *A)* Control (*i.e.*, YFP) and EGFR-expressing (EGFR) NMuMG cells were incubated in the absence (Pre-EMT) or presence (Post-EMT) of TGF-β1 (5 ng/ml) 24 h, at which point they were processed for E-cadherin (E-cad) and DAPI immunofluorescence (400x). Junctional localization of E-cadherin was slightly disrupted in EGFR-expressing NMuMG cells as compared to their control counterparts, except for regional pockets of cells designated by *white outline.* Delocalized and degradation of E-cadherin in response to TGF-β was enhanced in EGFR expressing cells. *B)* EGFR-expressing cells were stimulated to undergo EMT as in panel *A*, at which point they were subjected to dual immunofluorescent staining to visualize E-cadherin (E-cad, *red*) and EGFR (*green*). Regions lacking EGFR expression (*white outline*) exhibit normal junctional localization of E-cadherin, while EMT induction resulted in the appearance two populations of NMuMG cells: one that was EGFR-positive and E-cadherin-negative (*) and a second that lacked expression of both EGFR and E-cadherin (*arrows)*. Photomicrographs (400x) presented in panels *A* and *B* are representative of three independent experiments.

Author Manuscript Author Manuscript Author Manuscript Author Manuscript

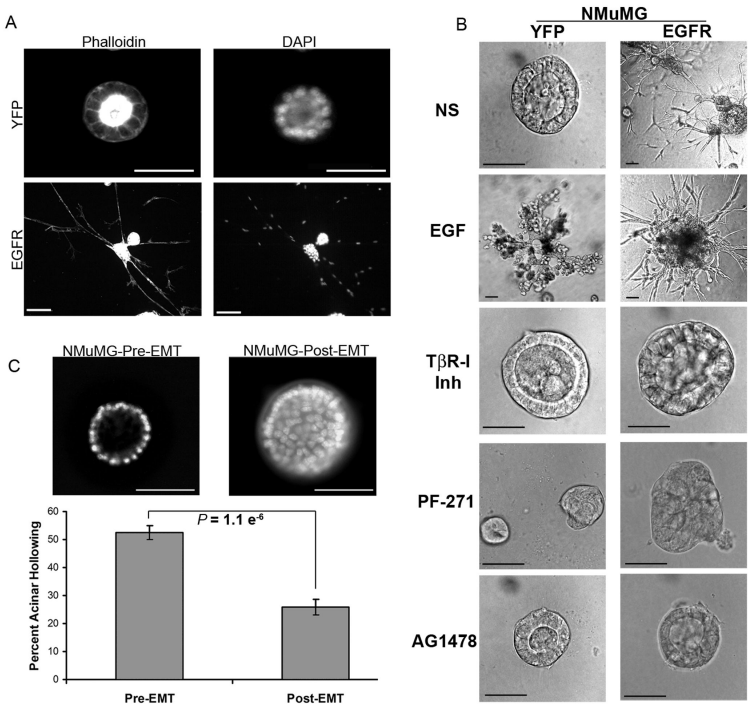

Figure 6.

MEC branching induced by EGFR is dependent upon TGF-β:FAK signaling. *A)* Control (*i.e.*, YFP) and EGFR-expressing (EGFR) NMuMG cells were propagated for 10 days in 3D-ogranotypic cultures, and subsequently were processed for direct phalloidin and DAPI fluorescence to visualize the actin cytoskeleton and nuclei, respectively. Shown are representative photomicrographs (YFP=400x; EGFR=100x) from a single experiment that was performed more than five times with identical results. *B)* Control (*i.e.*, YFP) and EGFR-expressing cells were propagated as in panel *A* in the absence (NS) or presence of either *a)* EGF (50 ng/ml); *b)* the TβR-I inhibitor, SB431542 (TβR-I inh, 10 μM); *c)* the FAK inhibitor, PF-562271 (PF-271, 1 μM), *d)* the EGFR inhibitor, AG1478 (1 μM). Shown are representative photomicrographs (small bar = 100x; large bar = 400x) from a single experiment that was performed at least 3 times with similar results. *C)* Parental NMuMG cells were incubated in the absence (Pre-EMT) or presence of TGF-β1 (5 ng/ml; Post-EMT) for 48 h prior to their isolation and propagation for 10 days in 3D-organotypic cultures. Afterward, the resulting organoids were stained with DAPI to visualize the nuclei and the percentage of hollowed acini was quantified. Data are the mean (±SE; n=3) percent of hollowed acinar structures. Representative acini are shown.

Author Manuscript Author Manuscript Author Manuscript Author Manuscript

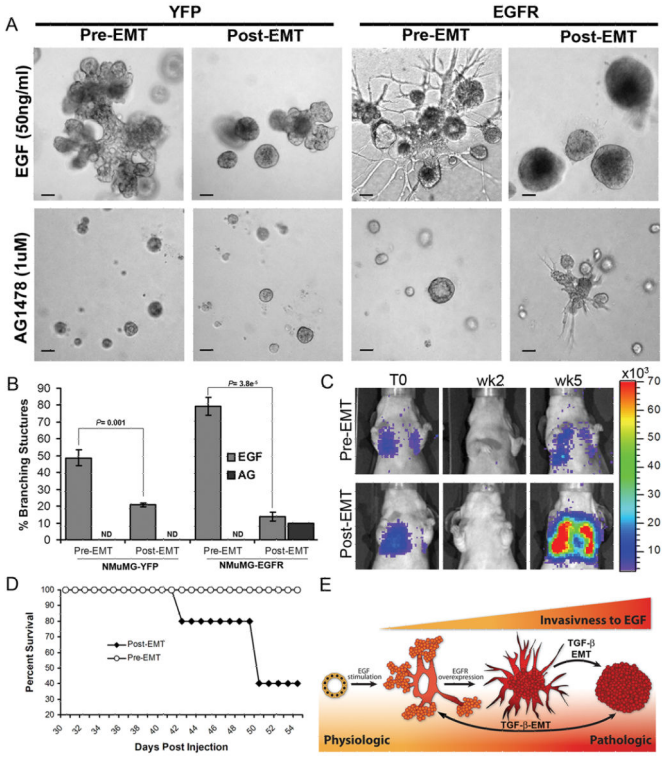

Figure 7.

EMT prevents EGF-induced mammary branching and increases pulmonary outgrowth. *A)* Control (*i.e.*, YFP) and EGFR-expressing (EGFR) NMuMG cells were incubated in the absence (Pre-EMT) or presence of TGF-β1 (5 ng/ml; Post-EMT) for 48 h prior to their isolation and propagation for 10 days in 3D-organotypic cultures supplemented with either EGF (50 ng/ml) or the EGFR antagonist, AG1478 (1 μM) as indicated. Differences in organoid morphology were monitored by phase-contrast microscopy (100x). *B*) Alterations in organoid branching were quantified and presented as the mean (±SE; n=3) percentage of branched structures. *C*) NMuMG-EGFR cells were transduced with firefly luciferase, treated with TGF-β1 as described in panel A and injected into the lateral tail vein of 6 week old, female, Nu/Nu mice. Shown is a longitudinal study of a representative mouse from each group imaged at the indicated time points (n=5 mice per group). *D*) A survival curve of mice injected with NMuMG-EGFR cells as in panel C, indicating that induction of EMT in NMuMG-EGFR cells decreases the time in which lethal pulmonary tumor burden is reached. *E*) Schematic depicts the relationship between MEC invasion, their EMT status induced by TGF-β, and their 3D-culture morphologies. In particular, EMT stimulated by TGF-β suppressed the branching of developing organoids including that induced by EGF/EGFR and instead resulted in the formation of large, dense spheroids that were hyper-invasive to EGF. This unique invasive morphology and phenotype is metastable (double-sided arrow) in normal mammary epithelial cells and required autocrine TGF-β signaling for its manifestation. In stark contrast, post-EMT invasospheres in mammary carcinoma cells are stabilized in their hyper-invasive phenotype (single-sided arrow) and hence rendered independent of the need for continued TGF-β stimulation. Our findings suggest that these

Author Manuscript Author Manuscript Author Manuscript Author Manuscript

novel invasive spheroids likely represent the post-EMT subpopulation of pathologically invasive and metastatic breast cancer cells.